proceedings

MDPI

Proceedings

Fluorinated and Platinized Titania for Glycerol Oxidation †

Edgar Bautista [1], Elsa G. Ávila-Martínez [2], Reyna Natividad [1], Julie J. Murcia [2,*], Rubi Romero [1], Jairo Cubillos [2], Hugo Rojas [2], Jhon S. Hernández [2], Oswaldo Cárdenas [3], María C. Hidalgo [4], José A. Navío [4] and Ramiro Baeza-Jiménez [2]

[1] Centro Conjunto de Investigación en Química Sustentable UAEM-UNAM, Carr. Toluca-Atlacomulco Km 14.5, Unidad San Cayetano, Toluca 50200, Mexico; edgarbaup@gmail.com (E.B.); reynanr@gmail.com (R.N.); rubiromero99@gmail.com (R.R.)

[2] Grupo de Catálisis, Escuela de Ciencias Químicas, Universidad Pedagógica y Tecnológica de Colombia UPTC, Avenida Central del Norte, Tunja 150003, Boyacá, Colombia; elsa.avila@uptc.edu.co (E.G.Á.-M.); jairo.cubillos@uptc.edu.co (J.C.); hugo.rojas@uptc.edu.co (H.R.); jhon.hernandez01@uptc.edu.co (J.S.H.); ramirobaezajimenez@gmail.com (R.B.-J.)

[3] Grupo de Fisicoquímica molecular y modelamiento computacional, Escuela de Ciencias Químicas, Universidad Pedagógica y Tecnológica de Colombia, Tunja, Boyacá, Colombia; oswaldo.cardenasptc.edu.co

[4] Instituto de Ciencia de Materiales de Sevilla (ICMS), Consejo Superior de Investigaciones Científicas CSIC—Universidad de Sevilla, Calle Américo Vespucio 49, C. P., 41092 Seville, Spain; mchidalgo@icmse.csic.es (M.C.H.); navio@us.es (J.A.N.).

* Correspondence: julie.murcia@uptc.edu.co; Tel.: +57-310-572-8828

† Presented at the 2nd International Online-Conference on Nanomaterials, 15–30 November 2020; Available online: https://iocn2020.sciforum.net/.

Published: 15 November 2020

Abstract: In this work, catalysts based on TiO_2 modified by fluorination and platinum addition were prepared, these materials were evaluated in the glycerol oxidation. The materials were characterized by TEM, N_2 physisorption, XRD, UV-Vis DRS, XRF and XPS. It was found that fluorination led to increase the surface area of TiO_2, and by platinization treatment it was possible to obtain a high absorption in the visible region of the electromagnetic spectrum. From these improved properties, it was prepared 0.5 wt.% Pt-F-TiO_2 as the best catalyst for the obtention of the highest yield and selectivity towards glyceraldehyde (GAL). It was also observed that the increase of Pt content had a detrimental effect in the effectiveness of fluorinated Titania in the glycerol conversion. The fluorination and platinum addition modify some physicochemical properties of TiO_2, leading also to modify the reaction mechanism and selectivity during glycerol oxidation.

Keywords: glycerol; oxidation; Pt-F-TiO_2; glyceraldehyde; dihydroxyacetone

1. Introduction

Glycerol is the structural component of many lipids and it is also the main by-product in biodiesel industry. Due to the fastest-growing of worldwide biodiesel production, high amounts of glycerol are generated as well, and so, it is necessary to develop innovative applications to utilize the excess of glycerol.

The chemical structure of glycerol composed by two primaries and one secondary hydroxyl groups, turn glycerol into a versatile platform to prepare value-added compounds. Pagliaro et al. have described several studies in this topic, where was reported the successful production of 1,3-dihydroxyacetone and hydroxypyruvic acid via glycerol oxidation and the enhancement of the performance of cements by bioglycerol addition [1,2]. Kenar [3] has reported that glycerol oxidation

is a promising reaction to obtain different organic compounds; however, it is rather difficult to control the partial oxidation of glycerol. In order to improve that reaction, a number of metallic catalysts have been evaluated and currently, the main catalysts of interest appear to focus on carbon-supported platinum, palladium or gold; bimetallic catalysts such as Au-Pd and Au-Pt, have also been studied [4]. As a result, a wide range of activities and selectivities to glyceric acid, dihydroxyacetone, tartronic acid, and hydroxypyruvic acid, have been reported, mainly using aqueous glycerol solutions as raw material [5]. These results depend on catalytic particle size and on the experimental conditions. Many reports have shown that Au-based catalysts are selective to the primary hydroxyls and the highest selectivity to glyceric acid was found by using a 1 wt.% Au (5–50 nm)/graphite catalyst [6].

For several decades, photocatalysis has been widely recognized and used in different fields as an eco-friendly process. In this sense, TiO_2 is a well-known photocatalyst because of its chemical and photochemical stability, biological inertness, strong oxidizing power and low cost [7–10]; however, TiO_2 has several drawbacks in terms of electron–hole recombination, it is visible light inactive and it has limited surface area [11]. Thus, in order to improve the photocatalytic and physicochemical properties of titania, some modifications of this semiconductor are very necessary to do. Among such modifications, metal doping is an effective approach and Pt, Au, porperties Pd, Ni, Cu, and Ag are able to act as electron trapper to prevent electron–hole recombination, thus enhancing TiO_2 photocatalytic efficiency. Moreover, fluorination and sulfation are suitable treatments for the improvement of TiO_2 physicochemical properties. These treatments lead to increase the specific surface area and the absorption of TiO_2 in the visible region of the electromagnetic spectrum [7,12,13].

On the other hand, another important drawback of Titania is given by its difficult recovering after heterogeneous photocatalytic reactions, it is mainly due to the small particle size of this oxide [14]. Many researchers have been focused in the study of different alternatives for the photocatalytic material recovering, and some of the most commonly methods employed in order to solve this problem is filtration and TiO_2 immobilization over glass, raschig rings, Silica, stainless steel plates and clay minerals [14–16].

The aim of the present study was to improve the strong oxidizing power of TiO_2 via fluorination and incorporation of platinum for the glycerol oxidation reaction. The catalysts were characterized in terms of physical properties as well as in operational conditions.

2. Materials and Methods

2.1. Catalysts Preparation

Different series of catalyst were prepared by TiO_2 modification and the typical procedure employed is described as follows.

2.1.1. Lab Prepared TiO_2

TiO_2 was prepared by hydrolysis of 200 mL of titanium tetraisopropoxide (Aldrich, 97%) in isopropanol solution (1.6 M) by the slow addition of distilled water (isopropanol:water 1:1, *v*/*v*). The powder obtained by sol-gel method was labeled as sg-TiO_2 and it was recovered by filtration, drying at 110°C overnight and calcination at 650 °C for 2 h, 4 °C/min was employed as the heating rate.

Commercial TiO_2 P25 Evonik (TiO_2 (C)) was used as the reference material with no additional pretreatment.

2.1.2. Fluorinated TiO_2

sg-TiO_2 material was pretreated by fluorination procedure to obtain fluorinated TiO_2 (F-TiO_2), this material was prepared by using an aqueous suspension of fresh sg-TiO_2 (2 g) in 1 L of 10 mM NaF; in order to maximize the fluoride adsorption, the pH was adjusted to 3 by using a solution 1 M of HCl [12,13]; this suspension was stirred for 1 h in the dark. After fluorination the powders were recovered by filtration, dried and calcined at 650 °C for 2 h, 4 °C/min was used as the heating rate.

2.1.3. Platinum Nanoparticles Photodeposition

Platinum (Pt) photodeposition over the calcined F-TiO_2 powders was carried out by using Hexachloroplatinic acid (H_2PtCl_6, Aldrich 99.9%) as metal source. Firstly, a suspension of the F-TiO_2 sample in distilled water containing 0.3 M of isopropanol (Merck 99.8%) as electron donor, was prepared. This suspension also contained the appropriate amount of metal precursor to obtain nominal platinum loading of 0.5 and 2 wt.% total of TiO_2. Pt photodeposition was then performed under continuous N_2 flux (0.90 L/h), by illuminating the suspension for 120 min. Light intensity on the suspensions was 60 W/m^2 determined by a photo-radiometer Delta OHM, HD2102.1. An Osram Ultra-Vitalux lamp (300 W), which possesses a sun-like radiation spectrum with a main emission line in the UVA range at 365 nm, was used as the light source. After photodeposition, the powders were recovered by filtration and dried at 110 °C for 12 h. The catalysts thus obtained, were labeled as 0.5 Pt-F-TiO_2 and 2 Pt-F-TiO_2.

2.2. Catalysts Characterization

Platinum particle sizes and morphology were evaluated by transmission electronic microscopy (TEM) in a Philips CM 200 microscope. For these analyzes, the samples were dispersed by sonication in ethanol and dropped on a carbon grid. The metal particle average diameter ($\bar{d}$) was determined by counting particles in a high number of TEM images from different places of the samples. The Equation (1) was used,

$$(\bar{d}nm) = \Sigma di \times fi \quad (1)$$

where di is the diameter of the ni counted particles and fi is the particle size distribution estimated by:

$$fi = ni/(\sum ni) \quad (2)$$

where ni is the number of particles of diameter di.

Specific surface area (S_{BET}) measurements were carried out by using low-temperature nitrogen adsorption in a Micromeritics ASAP2010 equipment. For this analysis the degasification of the samples was performed at 150 °C.

XRD analyzes were performed on a Siemens D-501 diffractometer with a Ni filter and graphite monochromator using Cu Kα radiation. Anatase crystallite sizes were calculated from the line broadening of the main anatase XRD peak (101) by using the Scherrer equation. Peaks were fitted by using a Voigt function.

In order to analyze the light absorption properties of the catalysts, these materials were evaluated by UV-Vis spectrophotometry. The UV–Vis DR spectra were recorded on a Varian spectrometer model Cary 100 equipped with an integrating sphere and using $BaSO_4$ as reference. Band-gap values of the samples were calculated by using the Kubelka–Munk functions, F(R∞), which are proportional to the absorption of radiation by plotting $(F(R\infty) \times hv)^{1/2}$ against hv [17].

The total Pt content and chemical composition of the catalysts synthesized were determined by X-ray fluorescence (XRF) in a PANalytical Axios sequential spectrophotometer equipped with a rhodium tube as the source of radiation. XRF measurements were performed on pressed pellets (sample included in 10 wt.% of wax).

X-ray photoelectron spectroscopy (XPS) studies were also carried out by using a Leybold–Heraeus LHS-10 spectrometer, working with constant pass energy of 50 eV. The spectrometer main chamber worked at $<2 \times 10^{-9}$ Torr, this equipment includes an EA-200MCD hemispherical electron analyzer with a dual X-ray source working with Al Kα (hv = 1486.6 eV) at 120 W and 30 mA. Before the XPS analyzes the samples were outgassed in the prechamber of the instrument at 150 °C up to a pressure $<2 \times 10^{-8}$ Torr to remove chemisorbed water. C 1s signal (284.6 eV) was used as internal energy reference in all the experiments.

2.3. Catalytic Tests

All catalysts were tested in the glycerol oxidation by using an experimental setup consisted of an open glass cylindrical reactor (2 cm id, 20 cm height) fitted with a cooling jacket. A 8 W lamp provided the UV light with a main emission at 254 nm, which was set inside the reactor; the energy source was a UVP PS-1 of 115 V/60 Hz and 40 A. In order to guarantee the continuous stirring and the homogeneity of the reaction mixture, a stirrer plate (Thermo Scientific) was set under the reactor. All these trials were carried out in batch mode. The bare and modified assessed catalysts were TiO_2(C), sg-TiO_2, F-TiO_2, 0.5 Pt-F-TiO_2 and 2 Pt-F-TiO_2 which were immersed in 100 mL of an aqueous glycerol (J.T. Baker, 99.7%) solution (100 mM). For the glycerol oxidation reaction, natural room oxygen was employed and the operational parameters evaluated were: platinum loading (0.5 and 2 wt.%) and catalyst amount (10, 30 and 40 mg). Catalytic reactions were carried out at outside room temperature with an average value or 19 °C and at starting pH value of 7.8. Blank tests without catalysts powders were also performed. In order to ensure the reproducibility of the results all the reactions were performed by duplicate.

At the end of the reaction cycle, the catalytic materials were recovered by filtration (0.45 μm filter), this procedure allowed us to recover 90% of the catalyst employed in the starting time of the glycerol oxidation reaction.

2.4. Oxidation Products Analysis

1.5 mL of sample were withdrawn from the liquid phase at selected times (0, 5, 10, 15, 30, 60, 120, 180, 240 and 300 min). In order to recover the catalytic materials, these samples were firstly filtered by using a Sartorius Biolab filters with a pore size of 0.45 μm and further analyzed by High Performance Liquid Cromatography (HPLC) and Total Organic Carbon (TOC). For HPLC analysis, 20 L of filtered samples by using Nylon Acrodisc Syringe Filters (diameter 25 mm and pore size of 45 μm), were injected and then measured in a SHIMADZU Model LC-2030 chromatograph. For these analyzes the next experimental conditions were employed: An UV 210 nm detector, a SiliaChrom SB C18 column (250 mm length × 5 mm internal diameter × 5 μm Film thickness), 45 °C, H_2SO_4 (aq) 0.01 mM was used as the mobile phase, total flow of 0.5 mL/min and total elution time of 10 min.

Aqueous solutions of Glycerol (G) J.T. Baker, 99.7%, Glyceraldehyde (GAL) Sigma-Aldrich, >90%, Dihydroxyacetone (DHA) Sigma-Aldrich 97%, Glycolic acid (GA) Sigma-Aldrich, 70 wt.% in water and Formic acid (FA) Honeywell >98%, were employed as HPLC standards. In order to determine the concentration of these compounds an integration of the data by using the Prominence I de SHIMADZU Labsolutions software was performed. Robustness, precision and accuracy studies were also carried out, from these studies it was possible to calculate a variation coefficient lower than 2%, showing the reliability of the measuraments. Other parameters such as conversion, yield and selectivity were also determined by using the equations enlisted as follows:

$$\text{Conversion (\%)} = (\text{Initial concentration of Glycerol} - \text{Final concentration of Glycerol})/(\text{Initial concentration of Glycerol}) \times 100 \quad (3)$$

$$\text{Yield (\%)} = (\text{Product concentration})/(\text{Initial concentration of Glycerol}) \times 100 \quad (4)$$

$$\text{Selectivity (\%)} = \text{Yield}/(\text{Glycerol conversion}) \times 100 \quad (5)$$

For TOC analysis, 100 L of filtered samples were measured in an Analytikjena Multi N/C 2100/1 equipment, by using a furnace temperature of 750 °C. Three measurements were performed for each sample and the average value was considered. Catalysts recycling experiments did not perform, it was mainly due to the low catalyst loading employed in our work (10, 30 or 40 mg); the loss of almost 10% of catalytic material in each test, makes non-viable this kind of experiments. However, it is interesting to abroad this analysis in a further research.

3. Results and Discussion

The present work describes an attempt to improve the catalytic activity of TiO_2 via combined fluorination and platinization for the selective oxidation of glycerol. The main results obtained from catalysts characterization and catalytic activity measurement are described as follows.

3.1. Platinum Particle Size

The morphology and Pt particle size distribution in the Pt-F-TiO_2 catalysts were analyzed by TEM and selected images are presented in Figure 1. As it can be observed, the platinum particles (small black spots) appear heterogeneously distributed on titania surface, with an average particle size of 6 nm for 0.5 Pt-F-TiO_2, the Pt particle size slightly increases with the platinum loading, thus, for the 2 Pt-F-TiO_2 phtocatalyst, Pt particles over 7 nm were observed. As it can also be observed in Figure 1, the Pt nanoparticles in 2 Pt-F-TiO_2 sample present higher degree of aggregation compared to its counterpart of 0.5 Pt-F-TiO_2.

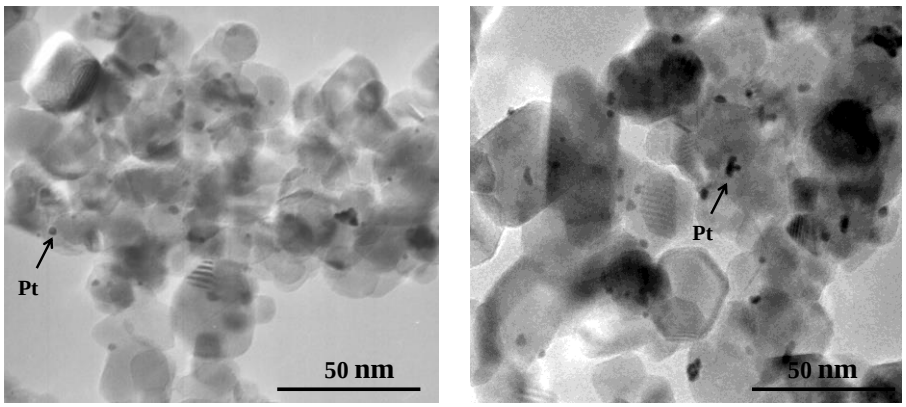

Figure 1. Selected TEM images of Pt-F-TiO_2 photocatalyst. (**Left**): 0.5 Pt-F-TiO_2 and (**Right**): 2 Pt-F-TiO_2.

3.2. Specific Surface Area

Table 1 summarizes the main physical characterization results for the commercial and lab prepared catalysts. Firstly, it is possible to observe an important difference between the specific surface area (S_{BET}) values in all the catalysts. Thus, the lowest value corresponds to 11 m^2/g in the sg-TiO_2 sample; this is mainly due to the titania particles sintering during the calcination process used in the preparation of this material at the lab. After fluorination, the S_{BET} value considerably increases, reaching almost the same S_{BET} value compared to the commercial Titania (i.e., 51 m^2/g). This result shows the protective effect of the fluorine ions over the surface area of TiO_2 at high temperature [8]. After platinum addition, it is observed that the specific surface area of fluorinated Titania (F-TiO_2) slightly decreases, which can be attributed to the obstruction of Titania surface as a result of the presence of platinum nanoparticles; this effect is less pronounced in the material prepared with the highest Pt loading, which can be explained taking into account that as it was observed by TEM analyzes previously described, the Pt particles present high size and high agglomeration degree, thus leading to a less obstruction of F-TiO_2 surface in comparison with the material prepared with low Pt content where a major number of metal nanoparticles of low size are covering the fluorinated Titania.

Table 1. Physical properties determined for N_2 physisorption, XRD, UV-Vis DRS and XPS for the photocatalysts assayed.

Photocatalysts	S_{BET} (m^2/g)	$D_{Anatase}$ (nm)	Band Gap (eV)	Binding Energy (eV)	
				Ti $2p_{3/2}$	O 1s
TiO_2 (C)	51	22	3.23	458.5	529.8
sg-TiO_2	11	17	3.30	458.5	529.8
F-TiO_2	51	24	3.21	458.4	529.6
0.5 Pt-F-TiO_2	42	23	3.24	458.3	529.6
2 Pt-F-TiO_2	50	22	3.26	461.3	531.2

3.3. Crystalline Phase Composition

The catalysts were also analyzed by XRD and it was found that both Rutile and Anatase crystalline phases are present in the TiO2 (C) and sg-TiO_2 samples, identified by the main XRD peaks located at 25.25° (JCPDS card no. 21-1272) and 27.44° (JCPDS card no. 21-1276), respectively (see Figure 2). Crystalline phases ratio was calculated from the intensity of the XRD peaks by using the method reported by H. Zhang et al. [15]; from these calculations the Anatase/Rutile ratio was found to be 90/10.

The presence of Rutile in the sg-TiO_2 may be associated with the titania particles sintering during the calcination at high temperature, thus leading to the rutilization and therefore to the lowest specific surface area observed in this sample. Only Anatase phase of TiO_2 was identified in the fluorinated and platinized samples, which is in agreement with previous results reported by different authors [11,18]; these authors have found that the addition of Fluorine ions on titania surface before calcination reduces the sintering of the particles, thus inhibiting the formation of Rutile phase. The Anatase crystallite size was also determined from the XRD spectra and the obtained values are reported in Table 1. As it can be seen, the sg-TiO_2 sample presents the lowest value corresponding to 17 nm. This could be related to the particle sintering coming from the formation of Rutile phase in this catalyst during the calcination process [12,13]. The highest Anatase crystallite size is observed in the fluorinated TiO_2; it has been reported that fluoride enhanced the crystallization of Anatase phase and promoted the growth of Anatase crystallites [11,18]. In the platinized sample, the Anatase crystallite size is very similar and no significant changes with the Pt addition were observed in this parameter.

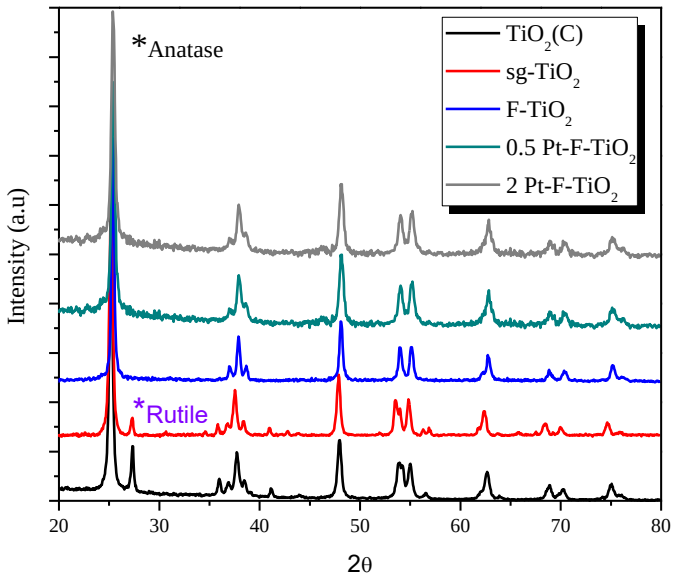

Figure 2. XRD patterns for bare and modified TiO_2 samples.

3.4. Optical Properties

The optical properties of the catalysts were analyzed by UV-Vis DRS and the spectra obtained are shown in Figure 3. The typical absorption band edge of the TiO_2 semiconductor was observed around 400 nm for all the samples. As it can be seen, the UV–Vis absorption of the fluorinated TiO_2 samples is slightly higher than that of the sg-TiO_2 sample; it can be due to the presence of fluoride species (Ti≡F) on TiO_2 surface. It can be also concluded that metallization did not substantially alter the absorption properties of the samples; however, an increase in absorption throughout the visible range of the spectrum was observed in Pt-F-TiO_2 samples; this is in concordance with the grey colour of these materials.

From the UV–Vis DR spectra, band gap energies were also calculated and the obtained results are reported in Figure 3 and Table 1, being 3.3 eV for the sg-TiO_2, after fluorination and/or platinization treatments a slight narrowing of the TiO_2 band gap was observed. The estimated band gap energies for the samples analyzed are between 3.21 and 3.26 eV, very close to that of Anatase TiO_2 (3.20 eV).

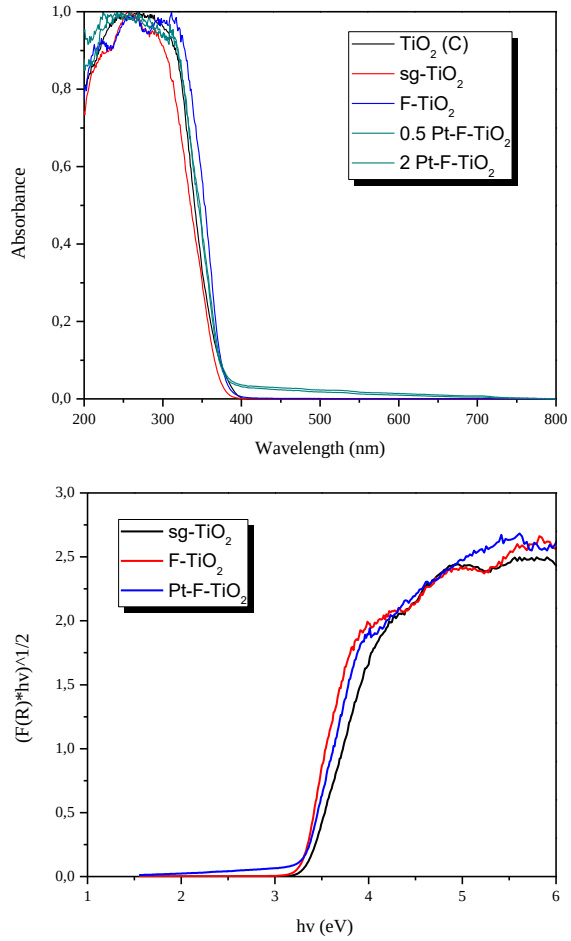

Figure 3. (**Up**): UV-Vis DR spectra of photocatalysts prepared and (**Down**): band gap calculation from Kubelka-Munk function.

3.5. Chemical Composition

The chemical composition of the catalysts was determined by XRF, from this technique, it was possible to detect traces of Cl^- species that remained from the metal precursor used in the preparation of the catalysts, in any case the chloride content exceeds 0.02%. Also the real platinum loading in the platinized samples was calculated by XRF and the obtained values are lower than the nominal metal content used to prepare the catalysts, thus indicating an incomplete reduction of the metal on the

TiO_2 surface during the photodeposition process. The amount of deposited Pt was close to 0.39 and 1.25 wt.% in the 0.5 Pt-F-TiO_2 and 2 Pt-F-TiO_2 samples, respectively.

3.6. XPS Analyzes

The results obtained by XPS are summarized in Table 1. The Ti 2p core peaks exhibit a main component at around 458.5 ± 0.1 eV (Ti $2p_{3/2}$) for all the catalysts, which is typical of the Ti4+ ions in the TiO_2 lattice. The addition of platinum did not modify the chemical environment of titanium atoms at the TiO_2 surface. In the O 1s region, a peak located at 529.8 ± 0.2 eV can be observed for all the samples, assigned to oxygen atoms in the TiO_2 lattice. This peak is asymmetric, with a shoulder at higher binding energies that can be ascribed to surface OH groups. By XPS analysis was also detected the presence of Na and fluoride species on the surface of the fluorinated samples, indicating that ≡$TiOH_2$ species could be substituted by ≡TiF [13,18]. By XPS it was also possible to observe that the Pt species have different oxidation states in the platinized samples, thus, reduced and oxidized species were detected in these samples, showing the incomplete metal reduction during the synthesis of the catalysts as it was also confirmed previously by XRF. Selected XPS spectra of the regions O 1s, Na 1s, F 1s and Pt 4f in the catalysts analyzed are shown in Figure 4.

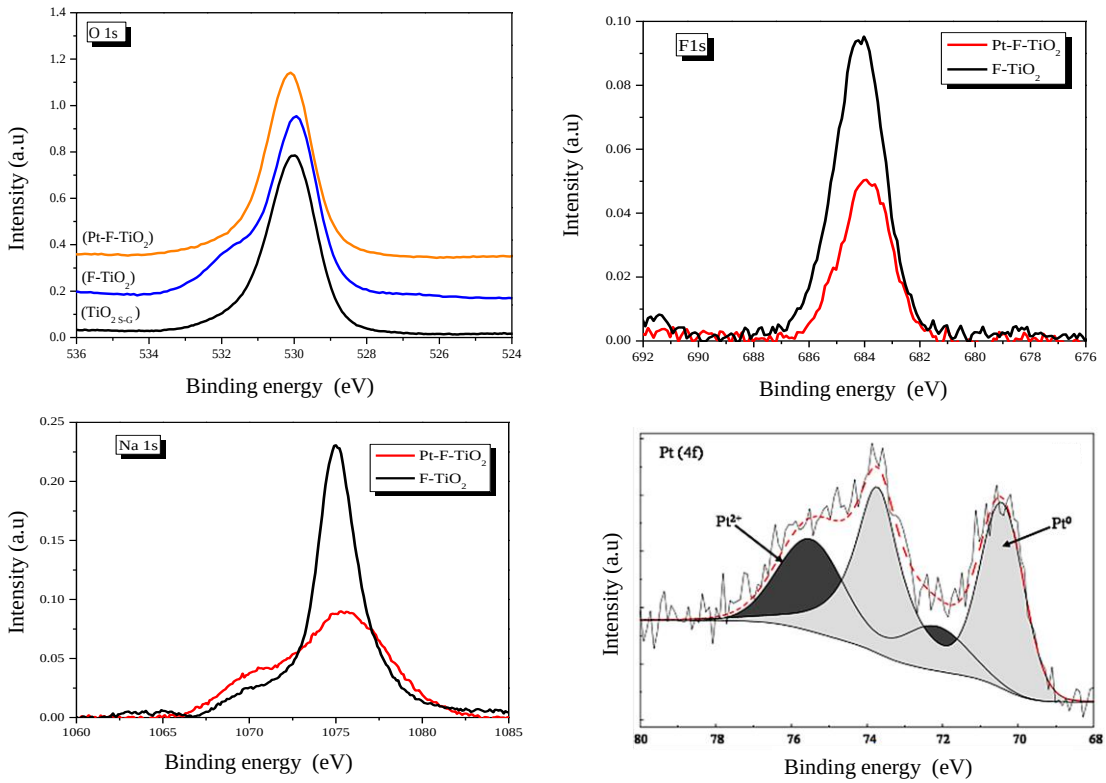

Figure 4. XPS spectra of the regions O 1s, Na 1s, F 1s and Pt 4f in the photocatalysts analyzed.

3.7. Catalytic Efficiency

As it was indicated in the experimental section, glycerol concentration and formation of reaction products were evaluated by HPLC. Figure 5 shows glycerol concentration as a function of the reaction time over each catalyst evaluated. As it can be noticed in this figure, the highest glycerol transformation was obtained in the blank test performed without catalyst powder, leading to obtain a final glycerol concentration of 11.4 mM after 300 min of reaction. The lowest glycerol transformation was obtained by using 2 Pt-F-TiO_2 as catalyst, it was 79.3 mM at the end of the reaction time.

As it was previously indicated, glycerol blank test was carried out and from the results obtained, it was noticed that glycerol is highly sensitive to be transformed by UV-Vis light into different compounds, it was also observed that the glycerol degradation increases with the illumination time,

thus leading to obtain a complex reaction mechanism, where almost 8 intermediaries compounds were identified. The catalytic performance was followed by measuring G, DHA, GAL and FA concentrations and calculating glycerol conversion, the yield and selectivities of the products (see Table 2).

Different tests without illumination and in presence of a catalys were also performed and no glycerol transformation was observed, only a slight reduction of this substrate concentration was detected, this is mainly due to the glycerol adsorption on catalysts surface.

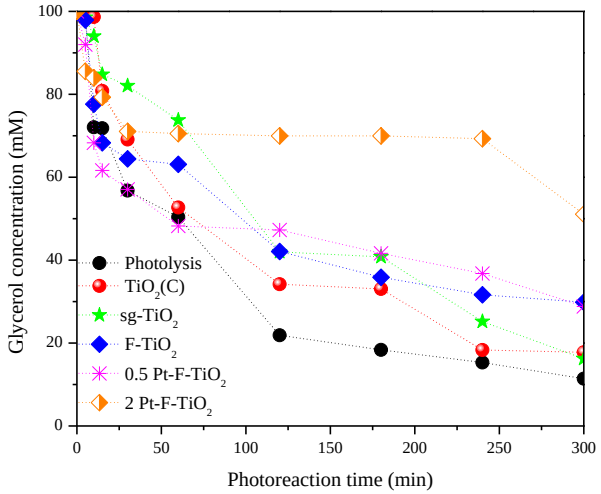

Figure 5. Glycerol concentration as a function of the reaction time over each photocatalyst evaluated.

Table 2. Conversion and yield calculated during the Glycerol oxidation after 300 min of reaction.

Photocatalyst	Glycerol Conversion (%)	GAL Yield (%)	DHA Yield (%)	FA Yield (%)	Other Products Yield (%)	GAL Selectivity (%)	DHA Selectivity (%)	FA Selectivity (%)	Other Products Selectivity (%)
Photolysis	88.40	0.12	6.60	12.80	68.90	0.13	7.51	14.50	77.90
TiO_2 (C) *	82.20	0.00	15.20	12.90	54.00	0	18.50	15.80	65.70
sg-TiO_2 *	83.50	0.00	15.16	21.24	54.7	0	16.64	23.31	49.87
F-TiO_2 *	69.40	0.00	9.23	60.20	0	0	13.30	87.00	0
0.5 Pt-F-TiO_2 *	57.40	30.40	24.91	2.10	0	52.98	43.39	3.63	0
2 Pt-F-TiO_2 *	20.40	12.03	0	8.33	0	59.10	0	40.83	0
0.5 Pt-F-TiO_2 (30 mg)	34.11	15.45	8.60	10.10	0	45.32	25.16	29.51	0
0.5 Pt-F-TiO_2 (40 mg)	14.83	14.83	0	0	0	0	0	0	0

On the other hand, all the catalysts synthesized were tested in the Glycerol oxidation (carried out under illumination) and it was found that the presence of a catalyst in the reaction medium highly modifies the reaction mechanism, thus leading to obtain different values of glycerol conversion and selectivity towards FA and DHA. The presence of the catalyst in the irradiated suspension reduce the number of photons absorbed by the glycerol, thus changing the sequence of chemical transformations occurring in this reaction. Hence, one should consider the kinetic aspect in the formation of certain chemicals. The reaction rate is reduced; henceforth certain reaction pathways start to prevail over the others leading to different distribution of reaction products.

The HPLC results obtained in the glycerol oxidation over some of the catalysts evaluated are represented in Figure 6. As it can be seen in this figure, by using lab prepared TiO_2 (Figure 6A) as catalyst, the glycerol starts to be transformed into FA at the first 15 min of reaction, then, DHA and other compounds are produced; a similar behavior it was observed by using commercial Titania. In the case of the lab prepared fluorinated Titania (F-TiO_2), the DHA and FA production was observed,

however, in this case no other compounds was detected (Figure 6B). Platinization of F-TiO_2 led to obtain also GAL (Figure 6C).

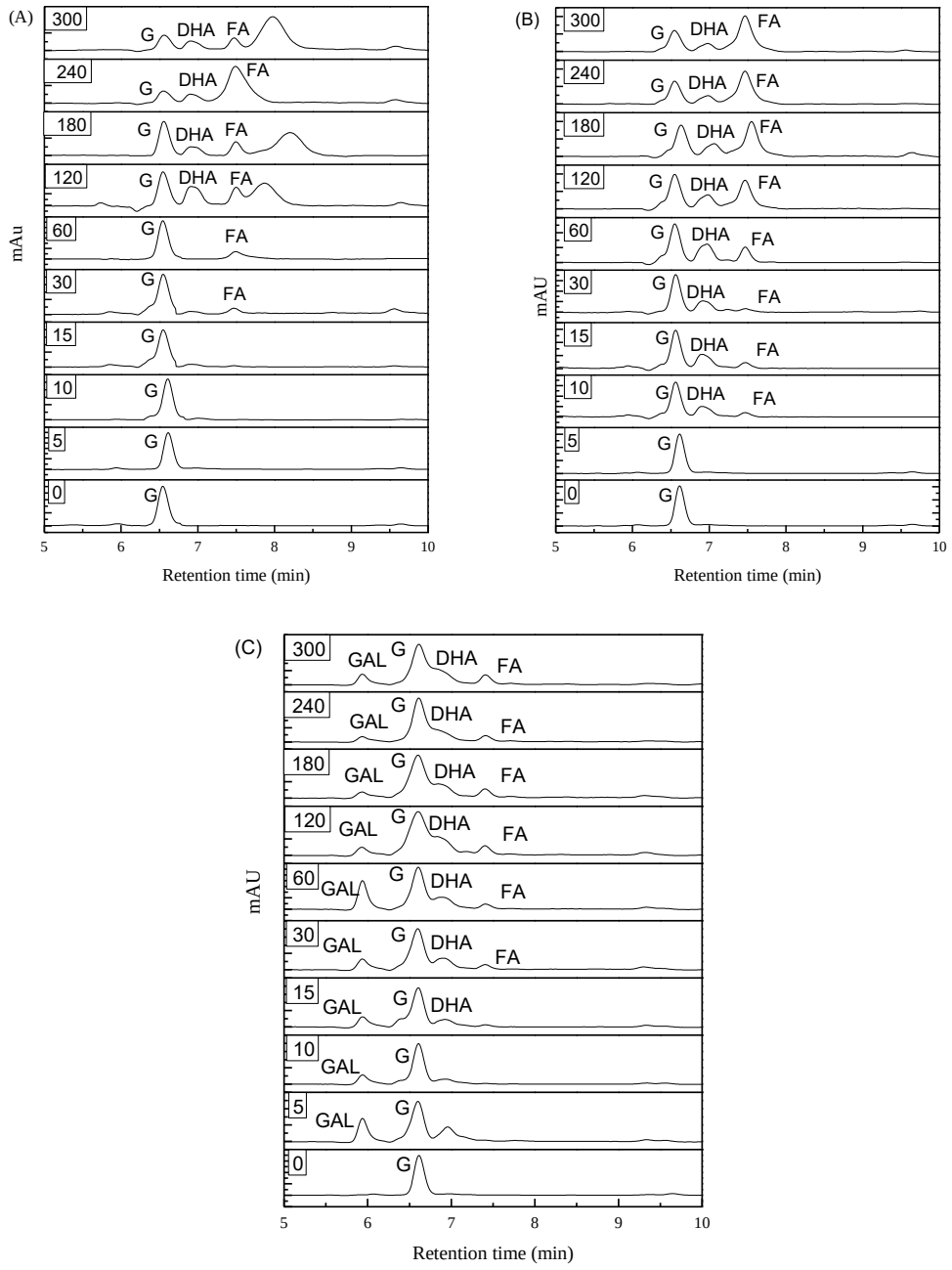

Figure 6. Glycerol photooxidation over the photocatalysts evaluated. (**A**) sg-TiO_2; (**B**) F-TiO_2 and (**C**) 2 Pt-F-TiO_2.

Table 2 includes a summary of the glycerol conversion, yield and selectivity results obtained during the glycerol oxidation after 300 min of reaction by using all the experimental parameters evaluated in the present work. As it can be seen, the highest glycerol conversion (88.4%) occurs during the blank test, this is due to the high number of intermediaries compounds formed as a consecuence of the illumination. It was also observed that commercial TiO_2 presents similar catalytic performance compared with its counterpart the lab prepared Titania.

With respect to the compounds of interest, GAL and DHA, the highest yields were achieved with the modified 0.5 Pt-F-TiO_2, indicating the potential of the prepared catalyst. Regarding

selectivity, it is also noted that 0.5 Pt-F-TiO_2 catalyst allows the formation of GAL. That can also be attributed to reaction mechanism occurring during glycerol oxidation.

It is interesting to note that as it can be clearly observed in Figure 6, over platinized and fluorinated Titania, firstly occurs a decrease of Glycerol concentration, but, after 50 min of reaction, the concentration of this substrate slightly increases, the same intermittent behavior is observed until the end of 300 min of total reaction time. These results can indicate that platinized catalysts present a highly reactive surface, thus over these materials, Glycerol oxidation can be a reversible reaction, where GLY can be transformed into other compounds, but from these new compounds also can be formed Glycerol again. These results can be explained taking into account that Pt nanoparticles can act as active sites on catalysts surface, in these sites Glycerol oxidation can occur but also this substrate can be efficiently adsorbed on positive Pt species; therefore, in the equilibrium of the reaction will coexist oxidative and reducing species that will define the course of the reaction according to the conditions in which it is produced.

3.7.1. Effect of the Platinum Loading

After Pt addition over F-TiO_2 it was observed a different behavior compared with the obtained by using the bare of fluorinated Titania in the glycerol oxidation, thus, only after platinization the formation of GAL was detected; it is also observed in Figure 6 that fluorination treatment and platinum addition inhibits the production of other compounds different from GAL, DHA and FA. Figure 7 shows the evolution of the glycerol oxidation products as a function of reaction time over sg-TiO_2 (Figure 7A), F-TiO_2 (Figure 7B), 0.5 Pt-F-TiO_2 (Figure 7C) and 2 Pt-F-TiO_2 (Figure 7D) catalysts.

It was also determined that the fluorination and the presence of Pt nanoparticles on F-TiO_2 decrease glycerol conversion, however, the Pt addition significantly increases the yield to GAL and DHA (Table 2). It is a relevant result, given the importance of these two compounds in different industrial activities, compared with FA; thus, DHA for example is used in the cosmetics industry as a tanning substance [2] and it is also useful as a monomer in polymeric biomaterials [19]; GAL is an intermediate of the carbohydrate metabolism and it is also a standard by which chiral molecules of the D- or L-series are compared [20].

However, it appears that the Pt loading has an important impact in the effectiveness of the F-TiO_2 in the glycerol oxidation, thus, with 0.5 Pt-F-TiO_2 catalyst a glycerol conversion value of 57.40%, a yield of 30.40, 24.91 and 2.1 to GAL, DHA and FA were obtained, respectively; however, by using the material prepared with 2 wt.% of Pt (2 Pt-F-TiO_2), the conversion and yield to the products in mention significantly decreases. This can be related to the glycerol adsorption on catalyst surface, thus, it is possible that Pt nanoparticles act as adsorption centers for glycerol, mainly taking into account that $Pt^{\delta+}$ species were identified by XPS analyzes in the platinized samples; these species can favor the adsorption of the strongly electronegative glycerol molecule. This hypothesis can be corroborated if it is observed that in the case of the 0.5 Pt-F-TiO_2 catalyst there are a high number of metal particles on surface compared with the 2 Pt-F-TiO_2 material, which can favor the substrate adsorption thus leading to a better oxidation. It can also be analyzed that in the 2 Pt-F-TiO_2 there are Pt particles with the highest size >7 nm; different authors have reported that larger Pt particle size is related to restricted absorption of substrate, thus, Liang et al. [21] have found that bigger sized Pt particles (>10 nm) were less active, smaller sized ones (<6 nm) exhibited higher glycerol conversion and stable selectivity; a similar behavior can occurs in the present work where the catalyst presenting the bigger Pt nanoparticles led to obtain the lowest performance in the glycerol oxidation.

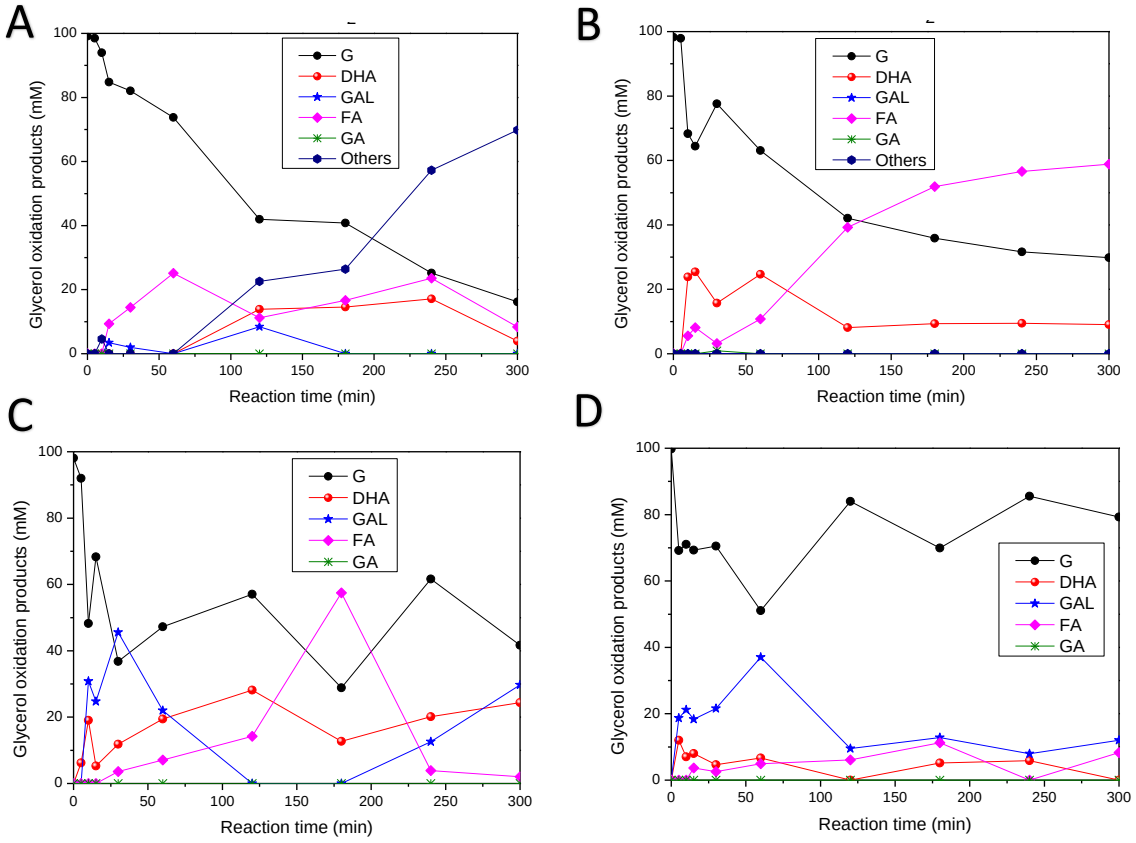

Figure 7. Glycerol and oxidation products concentration as a function of the photocatalytic oxidation time. (**A**) sg-TiO_2; (**B**) F-TiO_2; (**C**) 0.5 Pt-F-TiO_2 and (**D**) 2 Pt-F-TiO_2.

3.7.2. Effect of the Catalyst Amount

Taking into account that 0.5 Pt-F-TiO_2 catalyst shows the better performance and the highest GAL yield, this material was selected to test it in the glycerol oxidation reaction carried out by using different catalyst amount (i.e., 10, 30 and 40 mg). The results obtained are summarized in Table 2. As it can be seen, conversion and yield to the GAL, DHA and FA decreases as the catalyst amount increases, it can be due to that larger amounts of catalyst can increase the solution opacity and screening effects of particles can also occur, which mask part of the photosensitive area, thus leading to reduce the activity of the materials tested in the glycerol oxidation.

A preliminar study of the glycerol oxidation (evaluated by UV-Vis spectrophotometry) by using 10, 20 and 30 mg/L of 2% Pt-F-TiO_2, was also attempted. The results obtained have shown similar behaviour than that observed by using 0.5 Pt-F-TiO_2 catalyst, the best performance was observed by using 10 to 20 mg of catalyst loading per liter of glycerol solution.

3.8. Mineralization

In order to monitor the extent of the reaction, samples withdrawn from the fluid phase were analyzed by the Total Organic Carbon (TOC) method and the results obtained have been included in Figure 8. TOC results leads to conclude that mineralization was never reached. When the results obtained during the glycerol oxidation over Pt-F-TiO_2, using different catalyst loadings, slight changes can be observed for all the trials, but glycerol is not completely oxidized or mineralized in any case. This implies that CO_2 or H_2 were not produced. This effect was also observed when different catalyst amounts were tested with the other assessed materials.

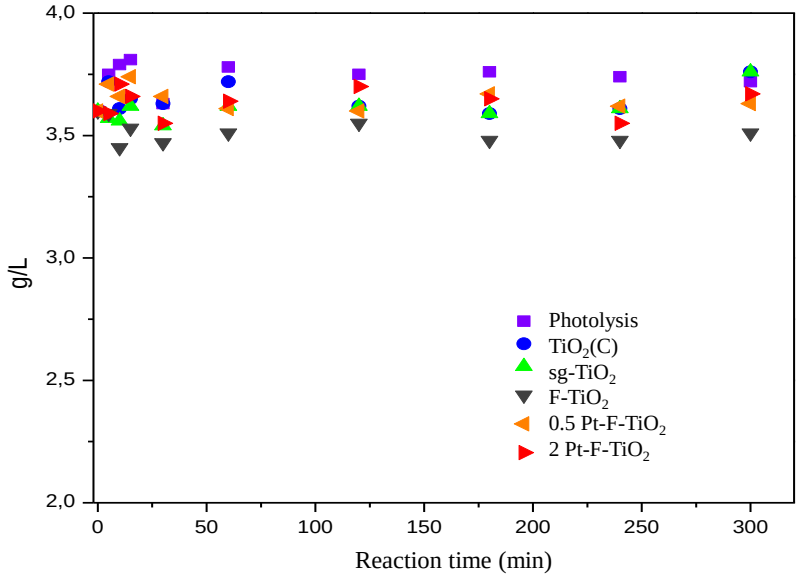

Figure 8. Total Organic Carbon (TOC) results as a function of the reaction time during the Glycerol oxidation over the photocatalysts analyzed.

4. Conclusions

Glycerol is sensitive to UV-Vis light, thus, it was observed that this molecule can be transformed under illumination giving rise to the formation of eight different compounds during the blank experiments, while in the presence of a catalyst in the reaction medium the number of products significantly decreases.

Fluorination and platinization lead to modify the optical and morphological properties of TiO_2 prepared by sol-gel method, thus leading to obtain a high absorption in the visible region and high surface area. It was observed that these treatments clearly modify the reaction mechanism and selectivity during glycerol oxidation reaction. Firstly, over commercial or lab prepared TiO_2 almost three intermediaries are produced after 60 min of reaction; after fluorine addition on TiO_2 surface, only the formation of DHA and FA was detected. Moreover, GAL, DHA and FA where observed when Pt was added.

Pt content and catalyst loading are key points influencing glycerol transformation effectiveness, thus, by increasing the Pt content from 0.5 to 2 wt.% glycerol conversion and therefore the intermediaries products yield decrease; it can be related to glycerol adsorption on Pt-F-TiO_2 surface, which is better on 0.5 wt.% Pt-F-TiO_2 catalyst. 10 mg was found to be the best loading for glycerol oxidation over 0.5 wt.% Pt-F-TiO_2, this amount is enough to allow the correct interaction between the catalyst and the substrate avoiding screening effect and low yields.

According to the results obtained it is worth noting that platinization is a suitable method to improve the F-TiO_2 efficiency in the glycerol tranformation into GCA and anyway the highest GAL production was obtained over 0.5 wt.% Pt-F-TiO_2 catalyst.

Author Contributions: J.J.M., R.B.-J.; R.N., and R.R., conceived and designed the experiments and looked for funding. J.J.M., J.S.H., O.C., E.G.Á.-M. and E.B. performed the experiments. J.J.M., J.S.H. and R.B.-J. analyzed the data and wrote the paper. H.R. and J.C. contributed reagents, materials and analysis tools. M.C.H. and J.A.N. performed the characterization analysis experiments. All authors have read and agreed to the published version of the manuscript.

Funding: This research was funded by Universidad Autónoma del Estado de México (UAEM), grant number 3892/2015 FS, by Fondo Nacional de Financiamiento para la Ciencia, la Tecnología y la Innovación Francisco José de Caldas—Colciencias, Project 279-2016 and Universidad Pedagógica y Tecnológica de Colombia grant SGI 2006.

Acknowledgments: Authors thanks to Universidad Autónoma del Estado de México (UAEM), grant number 3892/2015 FS, this work was also financed by Fondo Nacional de Financiamiento para la Ciencia, la Tecnología y la Innovación Francisco José de Caldas—Colciencias, Project 279-2016 and Universidad Pedagógica y Tecnológica de Colombia.

Conflicts of Interest: The authors declare no conflict of interest.

References

1. Rossi, M.; Della Pina, C.; Pagliaro, M.; Ciriminna, R.; Forni, P. Greening the Construction Industry: Enhancing the Performance of Cements by Adding Bioglycerol. *ChemSusChem* **2008**, *1*, 809–812, doi:10.1002/cssc.200800088.
2. Ciriminna, R.; Palmisano, G.; Della Pina, C.; Rossi, M.; Pagliaro, M. One-pot electrocatalytic oxidation of glycerol to DHA. *Tetrahedron Lett.* **2006**, *47*, 6993–6995, doi:10.1016/j.tetlet.2006.07.123.
3. Kenar, J.A. Glycerol as a platform chemical: Sweet opportunities on the horizon? *Lipid Technol.* **2007**, *19*, 249–253, doi:10.1002/lite.200700079.
4. Bowker, M.; Morton, C.; Kennedy, J.; Bahruji, H.; Greves, J.; Jones, W.; Davies, P.; Brookes, C.; Wells, P.; Dimitratos, N. Hydrogen production by photoreforming of biofuels using Au, Pd and Au–Pd/TiO_2 photocatalysts. *J. Catal.* **2014**, *310*, 10–15, doi:10.1016/j.jcat.2013.04.005.
5. Demirel-Gülen, S.; Lucas, M.; Claus, P. Liquid phase oxidation of glycerol over carbon supported gold catalysts. *Catal. Today* **2005**, *102*, 166–172, doi:10.1016/j.cattod.2005.02.033.
6. Ketchie, W.C.; Murayama, M.; Davis, R.J. Selective oxidation of glycerol over carbon-supported AuPd catalysts. *J. Catal.* **2007**, *250*, 264–273, doi:10.1016/j.jcat.2007.06.011.
7. Maicu, M.; Hidalgo, M.; Colón, G.; Navío, J.A. Comparative study of the photodeposition of Pt, Au and Pd on pre-sulphated TiO_2 for the photocatalytic decomposition of phenol. *J. Photochem. Photobiol. A Chem.* **2011**, *217*, 275–283, doi:10.1016/j.jphotochem.2010.10.020.
8. Li, D.; Haneda, H.; Hishita, S.; Ohashi, N.; Labhsetwar, N.K. Fluorine-doped TiO_2 powders prepared by spray pyrolysis and their improved photocatalytic activity for decomposition of gas-phase acetaldehyde. *J. Fluor. Chem.* **2005**, *126*, 69–77, doi:10.1016/j.jfluchem.2004.10.044.
9. Okazaki, K.; Morikawa, Y.; Tanaka, S.; Tanaka, K.; Kohyama, M. Effects of stoichiometry on electronic states of Au and Pt supported on TiO_2 (110). *J. Mater. Sci.* **2005**, *40*, 3075–3080, doi:10.1007/s10853-005-2667-3.
10. Mesa, J.J.M.; Romero, J.R.G.; Macías, Ángela, C.C.; Sarmiento, H.A.R.; Lobo, J.A.C.; Santos, J.A.N.; López, M.D.C.H. Methylene blue degradation over M-TiO_2 photocatalysts (M = Au or Pt). *Cienc. Desarro.* **2017**, *8*, 109–117, doi:10.19053/01217488.v8.n1.2017.5352.
11. Yu, J.; Xiang, Q.; Ran, J.; Mann, S. One-step hydrothermal fabrication and photocatalytic activity of surface-fluorinated TiO_2 hollow microspheres and tabular anatase single micro-crystals with high-energy facets. *Cryst. Eng. Commun.* **2010**, *12*, 872–879, doi:10.1039/b914385h.
12. Murcia, J.; Hidalgo, M.; Navío, J.; Araña, J.; Doña-Rodríguez, J. Study of the phenol photocatalytic degradation over TiO_2 modified by sulfation, fluorination, and platinum nanoparticles photodeposition. *Appl. Catal. B Environ.* **2015**, *179*, 305–312, doi:10.1016/j.apcatb.2015.05.040.
13. Iervolino, G.; Vaiano, V.; Murcia, J.; Rizzo, L.; Ventre, G.; Pepe, G.; Campiglia, P.; Hidalgo, M.; Navio, J.A.; Sannino, D.; et al. Photocatalytic hydrogen production from degradation of glucose over fluorinated and platinized TiO_2 catalysts. *J. Catal.* **2016**, *339*, 47–56, doi:10.1016/j.jcat.2016.03.032.
14. Chong, M.N.; Vimonses, V.; Lei, S.; Jin, B.; Chow, C.W.; Saint, C. Synthesis and characterisation of novel titania impregnated kaolinite nano-photocatalyst. *Microporous Mesoporous Mater.* **2009**, *117*, 233–242, doi:10.1016/j.micromeso.2008.06.039.
15. Fernandez, J.M.; Kiwi, J.; Baeza, J.; Freer, J.; Lizama, C.; Mansilla, H.D. Orange II photocatalysis on immobilised TiO_2. *Appl. Catal. B Environ.* **2004**, *48*, 205–211, doi:10.1016/j.apcatb.2003.10.014.
16. Molinari, R.; Pirillo, F.; Falco, M.; Loddo, V.; Palmisano, L. Photocatalytic degradation of dyes by using a membrane reactor. *Chem. Eng. Process.* **2004**, *43*, 1103–1114.
17. Tandon, S.P.; Gupta, J.P. Measurement of Forbidden Energy Gap of Semiconductors by Diffuse Reflectance Technique. *Phys. Status Solidi B* **1970**, *38*, 363–367, doi:10.1002/pssb.19700380136.
18. Vohra, M.S.; Kim, S.; Choi, W. Effects of surface fluorination of TiO_2 on the photocatalytic degradation of tetramethylammonium. *J. Photochem. Photobiol. A Chem.* **2003**, *160*, 55–60, doi:10.1016/s1010-6030(03)00221-1.

19. Behr, A.; Eilting, J.; Irawadi, K.; Leschinski, J.; Lindner, F. Improved utilisation of renewable resources: New important derivatives of glycerol. *Green Chem.* **2008**, *10*, 13–30, doi:10.1039/b710561d.
20. Augugliaro, V.; El Nazer, H.H.; Loddo, V.; Mele, A.; Palmisano, G.; Palmisano, L.; Yurdakal, S.; El-Nazer, H.A. Partial photocatalytic oxidation of glycerol in TiO_2 water suspensions. *Catal. Today* **2010**, *151*, 21–28, doi:10.1016/j.cattod.2010.01.022.
21. Liang, D.; Gao, J.; Wang, J.; Chen, P.; Hou, Z.; Zheng, X. Selective oxidation of glycerol in a base-free aqueous solution over different sized Pt catalysts. *Catal. Commun.* **2009**, *10*, 1586–1590, doi:10.1016/j.catcom.2009.04.023.